Journal of the American Heart Association

ORIGINAL RESEARCH

Repolarization Dispersion Is Associated With Diastolic Electromechanical Discoordination in Children With Pulmonary Arterial Hypertension

Michal Schäfer, PhD; Benjamin S. Frank, MD; D. Dunbar Ivy, MD; Max B. Mitchell, MD; Kathryn K. Collins, MD; Pei-Ni Jone, MD*; Johannes C. von Alvensleben, MD*

BACKGROUND: Electromechanical dyssynchrony is a well described comorbidity in pulmonary arterial hypertension (PAH). ECG-derived measurements reflective of diastolic dysfunction and electromechanical imaging markers are yet to be investigated. In this study we investigated the ECG- derived marker of repolarization dispersion, interval between the peak and end of T wave (TpTe), in pediatric patients with PAH and left ventricular (LV) diastolic dysfunction.

METHODS AND RESULTS: We measured TpTe from a standard 12-lead ECG and in 30 children with PAH and matched control subjects. All participants underwent same-day echocardiography and myocardial strain analysis to calculate the diastolic electromechanical discoordination marker diastolic relaxation fraction. When compared with control subjects, patients with PAH had increased TpTe (93±15 versus 81±12 ms, P=0.001) and elevated diastolic relaxation fraction (0.33±0.10 versus 0.27±0.03, P=0.001). Patients with PAH with LV diastolic dysfunction had significantly increased TpTe when compared with patients with PAH without diastolic dysfunction (P=0.012) and when compared with control group (P<0.001). Similarly, patients with PAH with LV diastolic dysfunction had increased diastolic relaxation fraction when compared with PAH patients without diastolic dysfunction (P=0.007) and when compared with control group (P<0.001). A 10-ms increase in TpTe was significantly associated with 0.023 increase in diastolic relaxation fraction (P=0.008) adjusting for body surface area, heart rate, right ventricular volumes, and function.

CONCLUSIONS: Prolonged myocardial repolarization and abnormal LV diastolic electromechanical discoordination exist in parallel in children with PAH and are associated with worse LV diastolic function and functional class.

Key Words: diastolic dysfunction ■ discoordination ■ pulmonary hypertension ■ repolarization

Biventricular diastolic dysfunction is an increasingly recognized comorbidity in pulmonary arterial hypertension (PAH).[1–3] Recent studies suggest that electromechanical dyssynchrony and discoordination might be important contributors to the impaired myocardial relaxation in PAH.[1,4–7] Imaging based measurements of the right and left ventricular (RV and LV) systolic discoordination and dyssynchrony were successfully related to the functional status of patients with PAH[8,9] as well as their hemodynamic and clinical outcomes.[1,5] A novel approach combining ECG-derived measurements and non-invasive cardiac deformation imaging have been frequently used to comprehensively assess electro-mechanical coupling.[9–11] However, similar studies specifically focusing on diastolic function are yet to be investigated in congenital heart disease and PAH.

The time interval between the peak and end of T wave (TpTe) measured in the precordial leads has been

Correspondence to: Michal Schäfer, Heart Institute, Children's Hospital Colorado, 13123 E 16th Ave, Aurora, CO 80045-2560. E-mail: michal.schafer@cuanschutz.edu

*P. N. Jone and J. C. von Alvensleben are co-first authors.

For Sources of Funding and Disclosures, see page 10.

JAHA is available at: www.ahajournals.org/journal/jaha

CLINICAL PERSPECTIVE

What Is New?

- Children with pulmonary arterial hypertension have abnormal dispersion of repolarization as evaluated by ECG-derived interval between the peak and end of T wave and impaired diastolic discoordination.
- ECG-derived interval between the peak and end of T wave and echocardiographic diastolic relaxation fraction are associated independently of traditional predictors of clinical outcomes in patients with pulmonary arterial hypertension.

What Are the Clinical Implications?

- In addition to systolic mechanical ventricular interdependency, diastolic ventricular interdependency with electromechanical substrate might be contributing to the left ventricular dysfunction and overall clinical presentation of children with pulmonary arterial hypertension.

Nonstandard Abbreviations and Acronyms

DRF	diastolic relaxation fraction
LVDD	left ventricular diastolic dysfunction
PAH	pulmonary arterial hypertension
TpTe	interval between the peak and end of the T wave

identified as a marker of myocardial dispersion of repolarization independently associated with echocardiographic measurements of diastolic dysfunction.[10,11] PAH related fibrotic myocardial changes with excessive collagen deposition known to affect the RV and to a lesser degree also LV, alter the magnitude and direction of conduction velocities.[12–14] Additionally, PAH animal model reported on myocardial repolarization instability as demonstrated by impaired dispersion of action potential.[15] These changes lead to electromechanical discoordination manifested by impaired myofibril relaxation compromising the effective LV preload generation and contribute to the LV diastolic dysfunction (LVDD).[4,6] Importantly, the LV function including the diastolic discoordination has been well demonstrated to contribute to the PAH clinical presentation and functional outcomes.[1,16,17] Despite the importance of LV relaxation to functional capacity and outcomes in patients with PAH, there are no validated ECG markers associated with LVDD in this population.

Consequently, the primary aim of this report is to study the previously investigated ECG-derived marker of myocardial repolarization dispersion, TpTe, in pediatric patients with PAH and presumptive LVDD. Specifically, we sought to investigate (1) whether TpTe differs between the patients with PAH and healthy controls, (2) whether TpTe is associated with non-invasive imaging derived markers of LV diastolic discoordination, and (3) whether combined measurements of repolarization dispersion and myocardial diastolic discoordination associate with the PAH functional measurements. We hypothesized that both ECG-based and imaging-based measurements of diastolic dysfunction will be abnormal in patients with PAH and that these changes will be reflective of the overall disease severity.

METHODS

The data that support the findings of this study are available from the corresponding author upon reasonable request. This study was part of a prospective PAH clinical biomarker study identifying imaging indices in children with diagnosed PAH. We identified 30 (n=30) consecutive patients with PAH seen in the Pulmonary Hypertension Clinic at Children's Hospital Colorado from December 2017 to June 2020, who underwent comprehensive clinical evaluation including same-day echocardiography and ECG as well as right heart catheterization within 1 week of the clinical evaluation. The initial diagnosis of PAH was established after evaluation by our Pulmonary Hypertension Program, which included echocardiograms and a prior cardiac catheterization, according to accepted guidelines.[18,19] Control subjects matched by age, sex, and BSA were selected from the group of patients who were referred for evaluation of heart murmurs and chest pain and had normal echocardiograms and ECGs. Exclusion criteria consisted of (1) patients in whom echocardiographic images were of suboptimal quality for the myocardial deformation analysis and (2) patients with atrial fibrillation or flutter. This study was approved by the Colorado Multi-Institutional Review Board with an approved waiver of informed consent and all methods were performed in accordance with the guidelines and regulations outlined in the Declaration of Helsinki.

ECG Analysis

Electrical dyssynchrony and dispersion of repolarization were analyzed using previously reported protocols.[1,11] Briefly, 12-lead ECGs that were collected same day as echocardiogram as a part of prospective clinical follow-up were evaluated by an electrophysiology specialist (J.C. von Alvensleben) blinded to the severity of PAH, echocardiography findings, and clinical outcomes. The manual tracing analysis of the standard 12-lead ECG signals sampled using standard settings of 25-mm/s speed and 10-mm/mV

amplitude was performed with commercially available software (TraceMasterVue version C.02 or later, Philips, Netherlands). The filtering and signal acquisition settings were uniformly applied for the entire study. Systolic electrical dyssynchrony was evaluated by measuring the QRS duration sampled from multiple leads and normalized using a *z*-score system specific for age and sex categories based on a historical data set.[20] Systolic electrical dyssynchrony was then defined as QRS duration *z*-score ≥2. Repolarization dispersion was evaluated by measuring the time interval between the peak and end of the T wave (T_{peak}-T_{end}) typically referred as TpTe interval. TpTe interval is considered to be the most reflective marker of transmural and total dispersion of repolarization.[21,22] TpTe interval was measured using the best available method using the T-wave in lead V_5 or lead V_4 and V_6, respectively, if V_5 was not suitable for analysis.[11] T_{end} was defined as the intersection of the maximum negative slope of the descending portion of the T-wave and isoelectric line (Figure 1).

Echocardiography

Echocardiography was performed on all subjects using IE-33 (Philips Ultrasound, Bothell, WA) or Vivid E9 or E95 (GE Ultrasound, Milwaukee, WI) ultrasound systems. Images were digitally acquired using a standard protocol with appropriately sized transducers for patient size. All ventricular diastolic markers were acquired according to consensus-based recommendations of the American Society of Echocardiography.[23] Mitral valve inflow Doppler and annular tissue septal and lateral Doppler imaging velocities along with mitral valve deceleration time were sampled per our institutional protocol to assess diastolic dysfunction. The stage of LVDD was in each subject categorized using consensus recommendations.[23,24] 3DE RV data sets were digitally analyzed offline using commercially available software (4DRV-Function 2.0, TomTec, Germany) to generate RV functional indices automatically as described previously.[25] For the purposes of electromechanical discoordination analysis, short-axis images at the mid-papillary level were uploaded to an off-line workstation for the myocardial deformation analysis using the 2-dimensional speckle tracking software (2DCPA; TomTec, Germany).

Electromechanical Discoordination

Diastolic electromechanical discoordination was evaluated using diastolic relaxation fraction (DRF) in a similar fashion as described previously using a modified approach applying 6 myocardial segments from the mid-papillary level corresponding to American Heart Association segments 7–12 (Figure 2).[1,26] Myocardial segment specific circumferential strain and strain rate temporal time curves were exported from TomTec platform for further numerical analysis into custom-made MATLAB program (Mathworks, Nattick, MA). Originally described as an extension of systolic stretch fraction,[7,26] DRF uses myocardial segment-specific strain $\varepsilon(t)$ and strain rate $d\varepsilon(t)/dt$ signal curves to calculate the relative ratio of myocardial contraction defined by $d\varepsilon(t)/dt_-$ (negative strain rate) to myocardial relaxation $d\varepsilon(t)/dt_+$ (positive strain rate) within a defined period of the cardiac cycle. Both components were derived from the strain rate signal $d\varepsilon(t)/dt$ numerically as follows:

$$d\varepsilon(t)/dt_+ = max\,(0, d\varepsilon(t)/dt) \rightarrow d\varepsilon(t)/dt_- = min\,(0, d\varepsilon(t)/dt).$$

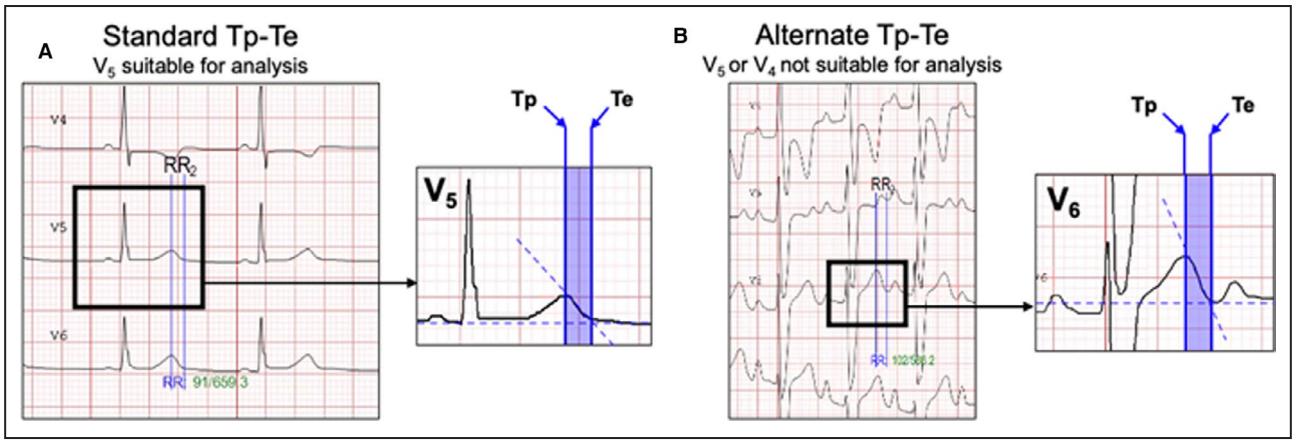

Figure 1. Schematic diagram representing T-wave analysis.
A, Interval between the peak and end of T wave analysis was performed using the best available method sampling the TpTe in lead V_5. **B**, If V_5 was not suitable for analysis, interval between the peak and end of T wave was recorded from V_4 or V_6 (in this order). T-end was defined as the intersection of the maximum negative slope of the descending portion of the T-wave and isoelectric line. TpTe indicates interval between the peak and end of T wave.

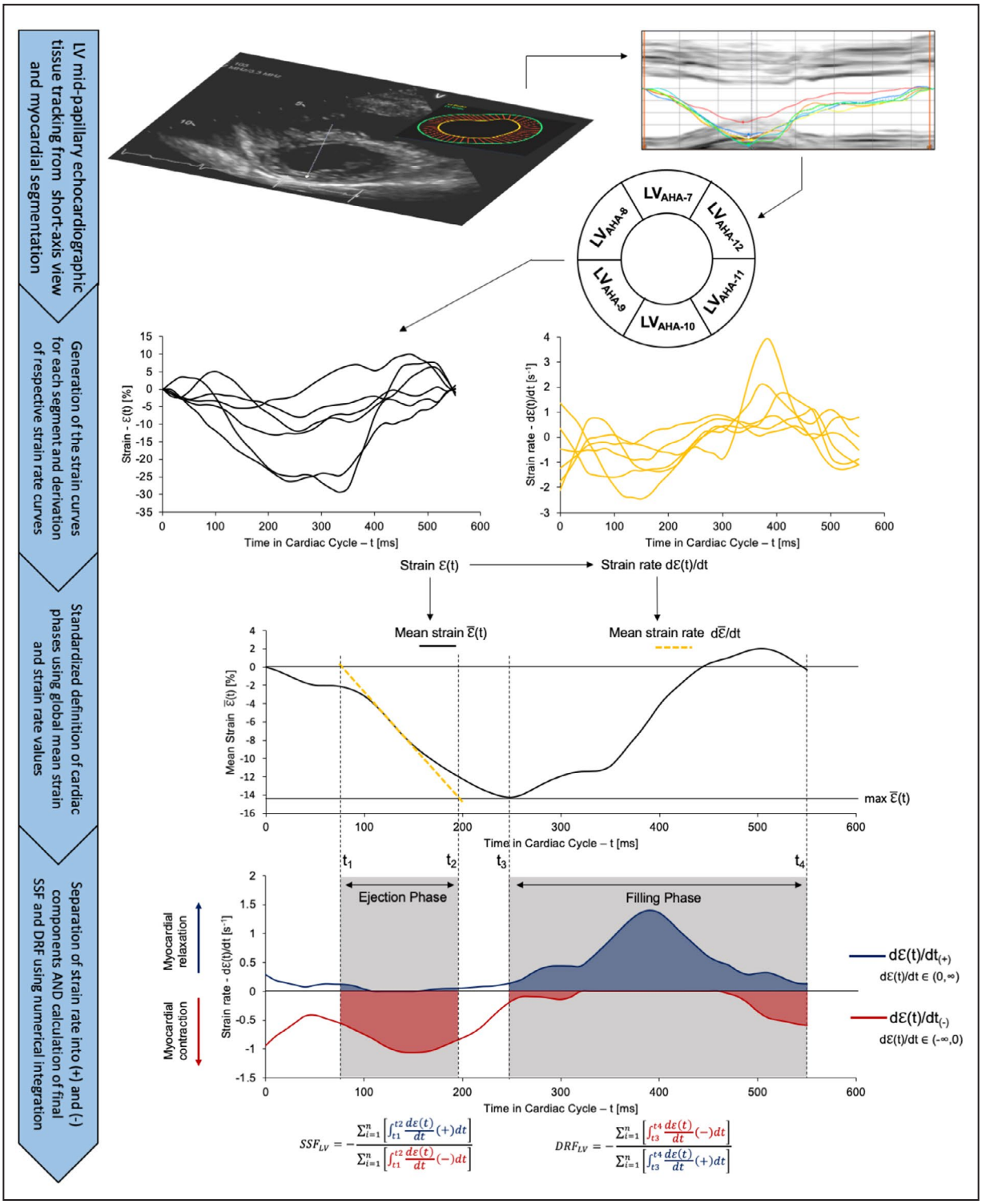

Figure 2. Schematic representing the analysis of electromechanical discoordination using the systolic stretch fraction (not analyzed in this study) and diastolic relaxation fraction.
Endocardial tracings of the left ventricular cavity from standard short-axis mid-papillary view were exported for further post-processing. Generated strain (black) and strain rate curves (yellow) representing 6 standardized American Heart Association segments were used to define myocardial filling phase and temporal boundary conditions for the calculation of diastolic relaxation fraction. The degree of inappropriate myocardial contraction during left ventricular filling phase was calculated as the ratio of area under the curve for segment specific negative strain rate (red line) and area under the curve of positive strain rate (blue line). AHA indicates American Heart Association; DRF, diastolic relaxation fraction; LV, left ventricular'; and SSF, systolic stretch fraction.

While the previously described systolic stretch fraction interrogates the ratio of myocardial contraction to the myocardial relaxation during ejection time from t_1 to t_2, DRF calculates the ratio of myocardial contraction to relaxation during the ventricular filling phase from time t_3 to t_4, and is mathematically defined as:

$$DRF = -\frac{\sum_{i=1}^{n}\left[\int_{t3}^{t4}\frac{d\varepsilon(t)}{dt}dt_{-}\right]}{\sum_{i=1}^{n}\left[\int_{t3}^{t4}\frac{d\varepsilon(t)}{dt}dt_{+}\right]}$$

where t_3 represents the time of the peak average circumferential strain, and t_4 represents the time at the end of the cardiac cycle. Increasing DRF values represent a higher proportion of contracting myocardial segments and therefore less efficient myocardial relaxation. The numerical analysis and the theory behind the calculation are described elsewhere.[1]

Statistical Analysis

Analyses were performed in Prism 9 or higher (GraphPad Software, La Jolla, CA, USA). Continuous variables were checked for the distributional assumption of normality using normal plots in addition to Kolmogorov–Smirnov and Shapiro–Wilks tests. Variables that were positively skewed (eg, NT-proBNP [N-terminal pro-B-type natriuretic peptide] and BNP values) were natural log-transformed for the correlative analyses. Demographic, hemodynamic, and clinical characteristics were compared between patients with PAH and healthy controls using Student *t*-test for normally distributed continuous variables, Mann-Whitney test for non-normally distributed variables, and $\chi 2$ for categorical variables. Results were displayed using Estimation plots for representation of the mean differences between groups. For descriptive and comparative purposes, the PAH patient population was subdivided into 2 groups by median TpTe interval (TpTe ≥92 ms versus TpTe <92 ms). Additional multiple group subanalyses (presence of LVDD, World Health Organization [WHO] functional class evaluation) were performed using 1-way ANOVA or Kruskal–Wallis tests with Tukey adjustment. Correction for multiple comparison (n=17 of statistical tests in Table 1 and n=19 of statistical tests in Table 2) was applied using Šidák and Bonferroni corrections. Interobserver variability of LV deformation measurements yielding DRF measure were assessed by 2 independent observers (M.S. and B.F.) in 10 randomly selected studies using intraclass correlation coefficient and Bland–Altman analysis. Good interobserver agreement between TpTe measurements with excellent intraclass correlation has been demonstrated previously.[11]

Univariate and multivariable linear regression models were applied to examine the associations between DRF, TpTe, RV function and volume, and PAH hemodynamic and functional outcomes unadjusted and adjusted for age, BSA, heart rate, and sex. Only the patient group was included into univariable and multivariable analyses to limit additional confounding similarly to previous studies.[1,11] Significance was based on an alpha-level <0.05.

RESULTS

Patient Population

Patient demographics, ECG parameters as well as PAH specific hemodynamics are summarized in Table 1. Sixteen patients had idiopathic PAH, 10 patients had PAH

Table 1. Demographics, ECG, Echocardiography

	PAH (n=30)	Control (n=30)	*P* value
Age, y	12.9±3.6	12.9±3.9	0.933
BSA, m^2	1.43±0.43	1.43±0.40	0.949
Sex (Female)	18 (60%)	18 (60%)	…
ECG			
QRS duration, ms	100±17	80±9	<0.001*
QRS z-score	1.3±1.4	−0.4±0.6	<0.001*
QT, ms	386±34	388±32	0.834
QTc, ms	427±19	456±27	<0.001
TpTe, ms	93±15	81±12	0.001*
Heart rate, bpm	84±15	68±13	<0.001*
LV echocardiography–diastolic indices			
DRF	0.33±0.10	0.27±0.03	0.005*
E-early inflow, m/s	0.85±0.20	0.92±0.16	0.104
A-early inflow, m/s	0.59±0.23	0.40±0.13	<0.001*
E/A	1.64±0.65	2.56±1.00	<0.001*
lateral e', cm/s	14.5±4.5	18.7±3.7	0.002*
E/e' (lateral)	6.6±3.4	4.9±1.3	0.012
RV Echocardiography			
RV EF 3D%	44±11	55±4	<0.001*
RV FAC (%)	36±12	40±3	0.040
RV EDVi, mL/m^2	111±65	52±16	<0.001*
RV ESVi, mL/m^2	68±23	57±7	<0.001*
mPAP, mm Hg	47±18		
PAWP, mm Hg	7±2		
PVRi, $WU.m^2$	11.3 (6.5–15.9)		
NT-proBNP, pg/mL	155 (84–324)		
BNP, pg/mL	41 (15–109)		
6MWT, m	500±70		

Data represented as mean±SD or median with corresponding interquartile range. (i) indicates index value to body surface area; 6MWT, 6-minute walk test; BNP, brain natriuretic peptide; BSA, body surface area; DRF, diastolic relaxation fraction; EDV, end-diastolic volume; EF, ejection fraction; ESV, end-systolic volume; FAC, fractional area change; LV, left ventricle; mPAP, mean pulmonary artery pressure; NT-pro BNP, N-terminal pro brain natriuretic peptide; PAH, pulmonary arterial hypertension; PAWP, pulmonary arterial wedge pressure; PVRi, pulmonary vascular resistance index; RV, right ventricle; and TpTe, interval between the peak and end of T wave.

*Comparison remains significant after adjustment for multiple correction.

Table 2. Characteristics by Repolarization Dispersion–TpTe Median

	TpTe ≤92 ms (n=17)	TpTe >92 ms (n=13)	*P* value
DRF	0.28±0.07	0.37±0.05	0.010
E-early inflow, cm/s	85±14	85±25	0.367
A-late inflow, cm/s	51±16	68±27	0.009
E/A	1.76±0.44	1.51±0.81	0.022
Heart rate, bpm	82±15	86±13	0.365
Septal e', cm/s	9.8±2.9	9.9±3.5	0.440
E/e' – Septal	9.4±3.5	9.6±3.8	0.690
Lateral e', cm/s	14.3±2.3	14.7±5.7	0.854
E/e' – Lateral	6.2±1.8	7.0±4.5	0.782
MVDT, ms	171±51	161±67	0.703
RV EF 3D%	45±9	44±14	0.336
RV FAC (%)	36±11	35±14	0.233
RV EDVi, mL/m^2	87 (74–104)	100 (68–178)	0.618
RV ESVi, mL/m^2	47 (33–56)	50 (37–133)	0.547
mPAP, mm Hg	50±16	44±21	0.476
PAWP, mm Hg	7±2	7±1	0.444
PVRi, WU.m^2	11.3 (7.8–18.1)	11.4 (5.1–18.2)	0.835
NT-proBNP, pg/mL	134 (73–234)	226 (93–2600)	0.195
BNP, pg/mL	33 (15–72)	109 (15–472)	0.324
6MWT, m	503±84	496±54	0.608

(i) indicates index value to body surface area; 6MWT, 6-minute walk test; BNP, brain natriuretic peptide; DRF, diastolic relaxation fraction; EDV, end-diastolic volume; EF, ejection fraction; ESV, end-systolic volume; FAC, fractional area change; mPAP, mean pulmonary artery pressure; MVDT, mitral valve deceleration time; NT-pro BNP, N-terminal pro brain natriuretic peptide; PAWP, pulmonary arterial wedge pressure; PVRi, pulmonary vascular resistance index; RV, right ventricle; and TpTe, interval between the peak and end of T wave.

associated with congenital heart disease, and 4 patients had hereditary familial form of PAH. Congenital heart defects included atrial septal defect (n=5), ventricular septal defect (n=3), and patent ductus arteriosus (n=2). All congenital defects were surgically corrected at the time of evaluation. Fourteen patients (47%) with PAH were categorized by echocardiographic criteria as having present LVDD. Three patients with PAH were classified as WHO-functional class I, 12 as class II, 12 as class III, and 3 as class IV. All patients were at the time of the evaluation receiving phosphodiesterase-5 inhibitors therapy, 19 patients were on endothelin receptor antagonists, and 17 patients were taking prostanoid analogues. Table 1 further summarizes diastolic LV echocardiographic measurements and 3-dimensional (3D) echocardiography indices reflective of RV hemodynamics. Patients with PAH had increased A-wave inflow velocity, reduced E/A ratio, and decreased lateral e' velocity, and increased E/e' ratio compared with controls. End-systolic and end-diastolic volume indices were increased when compared with controls while the RV ejection fraction and fractional area change were reduced.

ECG and Discoordination Biomarkers

When compared with control subjects, patients with PAH had increased QRS duration (100±17 versus 80±9 ms, Δ=20 ms, *P*<0.001), QRS z-score (1.3±1.4 versus −0.4±0.6, Δ=1.7, *P*<0.001), and increased TpTe time (93±15 versus 81±12 ms, Δ=12 ms, *P*=0.001) (Figure 3A through 3C). These results remained significant when patients with the right bundle branch block were excluded from the analysis. There was no difference in QT interval between both groups (386±34 versus 388±32, Δ=4 ms, *P*=0.834) but patients with PAH had decreased QTc (427±19 versus 456±27, Δ=29 ms, *P*<0.001). Two patients with PAH had right bundle branch block. DRF was significantly increased in patients with PAH compared with controls (0.33±0.10 versus 0.27±0.03, Δ=0.06, *P*=0.001) (Figure 3D). There was an excellent interobserver agreement with respect to the echocardiographic endocardial tracing yielding DRF measurements as demonstrated by mean DRF bias of 0.01 and intraclass coefficient of 0.95 (Figure 3E).

To evaluate the effect of LVDD present in patients with PAH, we performed a subanalyses comparing control subjects with patients with echocardiographic signs of LVDD and patients with PAH without echocardiographic signs of LVDD. PAH-LVDD group had significantly increased TpTe time when compared with patients with PAH without LVDD (*P*=0.012) and when compared with control group (*P*<0.001) (Figure 3F). However, there was no difference between patients with PAH without LVDD and controls (*P*=0.172). Similarly, the PAH-LVDD group had increased DRF when compared with patients with PAH without LVDD (*P*=0.007) and when compared with control group (*P*<0.001) (Figure 3G). There was no difference between patients with PAH with absent LVDD and controls (*P*=0.681). Additionally, patients with PAH with LVDD had increased heart rate when compared with PAH without LVDD (90±10 versus 77±15, Δ=13 ms, *P*=0.010) and when compared with controls (90±10 versus 68±10, Δ=22 ms, *P*<0.001).

Lastly, we performed a 3-group subanalysis between controls, patients with PAH with normal and mildly reduced functional status (WHO functional class I+II), and patients with PAH with moderately and severely reduced functional status (WHO functional class III+IV). The control group had significantly decreased TpTe when compared with patients with WHO functional class III+IV (*P*<0.001) but no further pair differences were observed (Figure 3H). Additionally, patients with PAH with WHO functional class III+IV had increased DRF when compared with controls (*P*<0.001) and when compared with WHO functional class I+II group (*P*=0.007) (Figure 3I). There was no difference between control group and WHO functional class I+II (*P*=0.642).

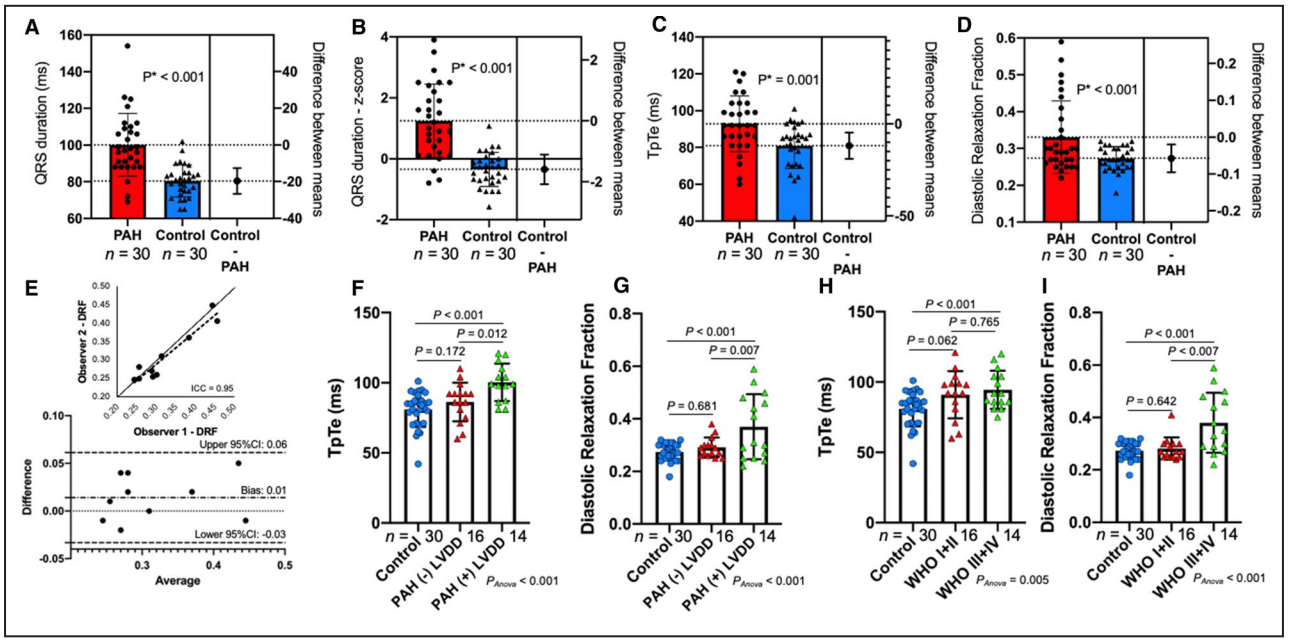

Figure 3. Comparison of ECG and myocardial deformation analysis.
A, QRS duration and (**B**) QRS duration z-score reflective of electrical dyssynchrony were increased in patients with pulmonary arterial hypertension compared with controls. **C**, Interval between the peak and end of T wave was increased in patients with pulmonary arterial hypertension. **D**, Diastolic relaxation fraction was correspondingly increased in pulmonary arterial hypertension group. **E**, Interobserver analyses concerning the diastolic relaxation fraction measurements. Subgroup analysis investigating the effect of left ventricular diastolic dysfunction presence on (**F**) interval between the peak and end of T wave and (**G**) diastolic relaxation fraction. Subgroup analysis investigating the severity of pulmonary arterial hypertension assessed by World Health Organization functional class on (**H**) interval between the peak and end of T wave and (**I**) diastolic relaxation fraction. DRF indicates diastolic relaxation fraction; LVDD, left ventricular diastolic dysfunction; PAH, pulmonary arterial hypertension; TpTe, interval between the peak and end of T wave; and WHO, World Health Organization.

Effect of TpTe on PAH Specific Biomarkers

To investigate the associations between TpTe, hemodynamics, and well-established prognostic markers in patients with PAH, we divided the PAH group by TpTe median (92 ms) for further comparison (Table 2). Patients with increased TpTe values had increased DRF, elevated A-inflow velocity, and lower E/A ratio (all $P<0.05$). There were no differences between the 2 groups in traditional tissue Doppler indices of LVDD as well as mitral valve deceleration time. Furthermore, there were no differences in 3D echocardiographic measurements of RV function and volume, and traditional outcome prognostic indices.

Association Between TpTe and DRF

To further explore the relationship between the dispersion of repolarization – TpTe and diastolic electromechanical discoordination – DRF, we performed univariable and multivariable regression analysis between TpTe and DRF (Table 3 and Figure 4A). In unadjusted analysis, each 10-ms increase in TpTe time was associated with 0.033 increase in DRF (P=0.003). In the final multivariable model we demonstrated the independent relationship between the TpTe and DRF after adjusting for BSA, heart rate, RV end-systolic and end-diastolic volumes, and RV function. In this final model, each 10-ms increase in TpTe was associated with 0.023 increase in DRF (P=0.008). Parallel increase in TpTe and DRF in different stages of LVDD is depicted in Figure 4B.

Table 3. Univariable and Multivariable Regression Between the DRF and TpTe

	β*±SE	95% CI	*P* value
Unadjusted	0.033±0.019	(0.011–0.055)	0.003
Model 1	0.033±0.010	(0.012–0.056)	0.003
Model 2	0.034±0.009	(0.014–0.053)	0.003
Model 3	0.023±0.008	(0.007–0.040)	0.008

Respective regression models are reported as β coefficients ± standard error and respective 95% CI. *β coefficients represent increase per 10-ms of interval between the peak and end of T wave, Model 1: adjusted for BSA, Model 2: adjusted for BSA and heart rate, Model 3: adjusted for BSA, heart rate, right ventricular ejection fraction, end-diastolic volume, and end-systolic volume. DRF, diastolic relaxation fraction; and TpTe, interval between the peak and end of T wave.

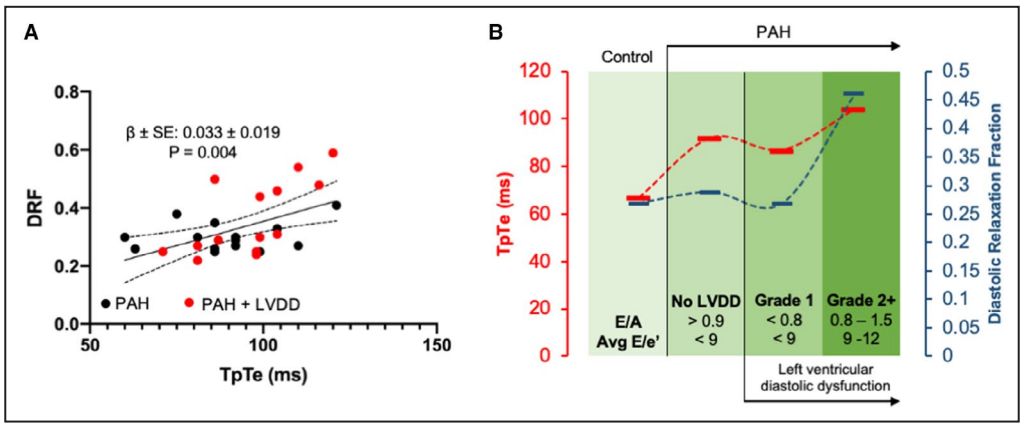

Figure 4. Relationship between interval between the peak and end of T wave and diastolic relaxation fraction.

A, Linear regression analysis between interval between the peak and end of T wave measurements and diastolic relaxation fraction. **B**, Evolution of average interval between the peak and end of T wave and diastolic relaxation fraction values in patients with pulmonary arterial hypertension subclassified by left ventricular diastolic dysfunction algorithm Average values for TpTe (red) and Diastolic Relaxation Fraction (blue) within each category. DRF indicates diastolic relaxation fraction; LVDD, left ventricular diastolic dysfunction; PAH, pulmonary arterial hypertension; and TpTe, interval between the peak and end of T wave.

DISCUSSION

LVDD is a significant comorbidity and prognostic biomarker in children with PAH.[1,27] The inter-ventricular dependency in patients with PAH has been demonstrated using mechanical and electrical dyssynchrony.[6,27,28] In this study, we demonstrated that children with PAH have (1) abnormal dispersion of repolarization as evaluated by TpTe, (2) impaired diastolic electromechanical discoordination as evidenced by elevated DRF, and (3) that ECG-derived TpTe and echocardiographic DRF are associated independently of traditional predictors of clinical outcomes in patients with PAH. These results suggest that impaired myocardial repolarization and inefficient LV relaxation may be contributing to the PAH comorbidities. Given that worse hemodynamic and clinical outcomes in patients with PAH are associated with impaired LV function,[16,28,29] the observed link between altered electrical and mechanical pathophysiology might provide important insights into overall disease progression.

Increasing evidence suggests that TpTe provides a more accurate representation of transmural myocardial repolarization dispersion than QT interval measurements.[21] Importantly, TpTe is consistently associated with imaging markers of myocardial deformation and standard echocardiographic measures of diastolic dysfunction.[10,11] In this study we found that TpTe was significantly elevated in children with PAH and was associated with the presence of LVDD. The observed relationship between TpTe and LV diastolic discoordination was significant independently of RV performance markers. Additionally, TpTe was significantly increased in patients with LVDD despite elevated heart rate suggesting that this measurement might be primarily influenced by the T-wave morphology, particularly by its end slope. PAH animal models demonstrated that electrical remodeling is responsible for biventricular conduction delays and impaired myocardial repolarization.[30,31] However, repolarization gradients are location and orientation dependent[22] and further studies considering additional lead-specific T-wave features might provide additional insights into ventricle specific diastolic dysfunction. The finding of a decreased QTc combined with a prolonged TpTe in patients with PAH is noteworthy and bears mentioning. Increased dispersion of repolarization is generally thought to predispose to ventricular arrhythmias and a shortened QT interval, implying a shortened duration of repolarization, may result in an increased arrhythmia risk. Our patient cohort did not demonstrate any sustained arrhythmias although detailed analysis of non-sustained ventricular arrhythmias is not possible secondary to inconsistent rhythm monitoring.

Prior studies investigating the electrical-mechanical coupling in PAH have naturally focused on the RV systolic performance using electrical dyssynchrony as an important biomarker reflective of patient functional status.[4,5,9] An accumulating body of evidence from pediatric focused studies suggests that right-to-left mediated ventricular interdependency is impacting both LV systolic and diastolic dysfunction.[6,27,28] More recently, Frank et al showed that LV diastolic electromechanical discoordination as measured by

DRF is associated with clinical worsening in children with PAH.[1] Our study further contributes to the aforementioned results by demonstrating that abnormal myocardial repolarization as evidenced by elevated TpTe is strongly associated with the LV specific DRF. DRF is arguably more reflective of electromechanical coupling than standard mechanical dyssynchrony indices such as time to peak measurements, because DRF considers the deformation state of each myocardial segment only with respect to the filling phase of cardiac cycle. Interestingly, a study by Spragg et al demonstrated that the presence of electrical and mechanical dyssynchrony in the LV with subclinical dysfunction induces regionally specific alterations in conduction and heterogenous repolarization.[32] In this and prior studies,[1,33] an applied DRF model has been limited only to 2-dimensional myocardial deformation using only a circumferential strain and strain rate. Therefore, the extension of myocardial electromechanical discoordination analysis might further require longitudinal and radial deformation indices to comprehensively appreciate diastolic electromechanical coupling. Expansion into 3-dimensional imaging techniques with corresponding motion analysis would further allow for more accurate myocardial deformation analysis accounting for through plane motion and overall cardiac displacement.

The ideal physiologic model of mechanical dyssynchrony or discoordination needs to separately investigate the electrical conduction, electro-mechanical coupling, and the final regional myocardial contractility. However, there is also a strong correlation between transmural repolarization and myocardial relaxation sequences suggestive of diastolic electromechanical coupling.[11,34] Therefore, studies combining simultaneous electrophysiologic mapping with imaging based myocardial discoordination analysis might provide additional insight into electro-mechanical systolic and diastolic coupling. The effect of impaired myocardial repolarization on preload generation has been previously demonstrated by association between observed T-wave changes and isovolumic relaxation time.[34] In our study, elevated TpTe was only associated with increased A-wave inflow velocity and reduced E/A ratio. However, standard echocardiographic Doppler and tissue-Doppler indices of LVDD have not been well validated in the pediatric setting.[23,35] Our future studies will focus on investigating the TpTe and DRF in context of LV filling pressures to fully explore the association between electromechanical coupling and diastolic dysfunction.

Limitations

We acknowledge several limitations associated with our study. First, the applied circumferential strain analysis only considered the LV mid-papillary level myocardium yielding 6 American Heart Association models serving as the input for DRF calculation. Given that this was the first study applying echocardiography derived DRF, we wanted to mitigate potential variability and poor imaging quality associated with basal and apical short-axis views. This approach showed an excellent inter-reader reproducibility but might benefit from extension into basal and apical regions as well as consideration of incorporating longitudinal deformation. Second, TpTe has been well associated with transmural repolarization dispersion[10,11,21] but might be less reflective of global repolarization.[22] Further exploration of TpTe combining T-wave analysis from other leads might be necessary to comprehensively evaluate the heterogeneity of repolarization. Third, our PAH patient population involved patients with repaired ventricular septal defect (n=3) in which conduction abnormalities might have been present as a result of the surgical intervention. None of the considered patients presented with QRS duration z-score >2 and all 3 belonged to the second tertile of measured TpTe duration. Our future investigations will involve larger patient population to more precisely elucidate the effect of idiopathic PAH on diastolic electromechanical coupling. Lastly, electrical dyssynchrony as evaluated by QRS duration and heart rate secondarily influence the pattern and duration of repolarization, respectively. We did not directly investigate the relationship between the electrical dyssynchrony markers and TpTe. Our future studies will investigate T-wave morphologic features and their association with other ECG based events.

CONCLUSIONS

Impaired myocardial repolarization and abnormal LV diastolic electromechanical discoordination exist in parallel in children with PAH and might contribute to the overall disease progression. Given the strong predictive value of LV function in patients with PAH, further investigations evaluating mechanistic relationship between RV dysfunction and LV diastolic electromechanical coupling warrant investigation. We propose that in addition to systolic mechanical ventricular interdependency, diastolic ventricular interdependency with electromechanical substrate might be contributing to the LV dysfunction and overall clinical presentation of children with PAH. Our future studies will investigate the prognostic potential of TpTe and DRF as well as their association with PAH-specific phenotypes.

ARTICLE INFORMATION

Received November 19, 2021; accepted January 24, 2022.

Affiliations

Division of Cardiology, Heart Institute, Children's Hospital Colorado, University of Colorado Denver, Denver, CO (M.S., B.S.F., D.D.I., K.K.C., P.-N.J., J.C.v.A.) and Section of Congenital Heart Surgery, Heart Institute, Children's Hospital Colorado, University of Colorado Denver, Anschutz Medical Campus, Aurora, CO (M.B.M.).

Sources of Funding

This work was supported by Rady Family and Jayden DeLuca foundations.

Disclosures

None.

REFERENCES

1. Frank BS, Schäfer M, Douwes JM, Ivy DD, Abman SH, Davidson JA, Burzlaff S, Mitchell MB, Morgan GJ, Browne LP, et al. Novel measures of left ventricular electromechanical discoordination predict clinical outcomes in children with pulmonary arterial hypertension. *Am J Physiol Circ Physiol*. 2019;318:401–412. doi: 10.1152/ajpheart.00355.2019
2. Vonk-Noordegraaf A, Haddad F, Chin KM, Forfia PR, Kawut SM, Lumens J, Naeije R, Newman J, Oudiz RJ, Provencher S, et al. Right heart adaptation to pulmonary arterial hypertension: physiology and pathobiology. *J Am Coll Cardiol*. 2013;62:D22–D33. doi: 10.1016/j.jacc.2013.10.027
3. Tji-Joong Gan C, Lankhaar J-W, Marcus JT, Westerhof N, Marques KM, Bronzwaer JGF, Boonstra A, Postmus PE, Vonk-Noordegraaf A. Impaired left ventricular filling due to right-to-left ventricular interaction in patients with pulmonary arterial hypertension. *Am J Physiol Circ Physiol*. 2005;290:H1528–H1533. doi: 10.1152/ajpheart.01031.2005
4. Badagliacca R, Reali M, Poscia R, Pezzuto B, Papa S, Mezzapesa M, Nocioni M, Valli G, Giannetta E, Sciomer S, et al. Right intraventricular dyssynchrony in idiopathic, heritable, and anorexigen- induced pulmonary arterial hypertension. *JACC Cardiovasc Imaging*. 2015;8:642–652. doi: 10.1016/j.jcmg.2015.02.009
5. Hill AC, Maxey DM, Rosenthal DN, Siehr SL, Hollander SA, Feinstein JA, Dubin AM. Electrical and mechanical dyssynchrony in pediatric pulmonary hypertension. *J Hear Lung Transplant*. 2012;31:825–830. doi: 10.1016/j.healun.2012.04.004
6. Schäfer M, Collins KK, Browne LP, Ivy DD, Abman S, Friesen R, Frank B, Fonseca B, DiMaria M, Hunter KS, et al. Effect of electrical dyssynchrony on left and right ventricular mechanics in children with pulmonary arterial hypertension. *J Hear Lung Transplant*. 2018;37:870–878. doi: 10.1016/j.healun.2018.01.1308
7. Kirn B, Jansen A, Bracke F, van Gelder B, Arts T, Prinzen FW. Mechanical discoordination rather than dyssynchrony predicts reverse remodeling upon cardiac resynchronization. *Am J Physiol Circ Physiol*. 2008;295:H640–H646. doi: 10.1152/ajpheart.00106.2008
8. López-Candales A, Dohi K, Rajagopalan N, Suffoletto M, Murali S, Gorcsan J, Edelman K. Right ventricular dyssynchrony in patients with pulmonary hypertension is associated with disease severity and functional class. *Cardiovasc Ultrasound*. 2005;3:23. doi: 10.1186/1476-7120-3-23
9. Badagliacca R, Papa S, Valli G, Pezzuto B, Poscia R, Reali M, Manzi G, Giannetta E, Berardi D, Sciomer S, et al. Right ventricular dyssynchrony and exercise capacity in idiopathic pulmonary arterial hypertension. *Eur Respir J*. 2017;49. doi: 10.1183/13993003.01419-2016
10. Sauer AJ, Selvaraj S, Aguilar FG, Martinez EE, Wilcox JE, Passman R, Goldberger JJ, Freed BH, Shah SJ. Relationship between repolarization heterogeneity and abnormal myocardial mechanics. *Int J Cardiol*. 2014;172:289–291. doi: 10.1016/j.ijcard.2013.12.232
11. Sauer A, Wilcox JE, Andrei AC, Passman R, Goldberger JJ, Shah SJ. Diastolic electromechanical coupling: association of the ECG T-peak to T-end interval with echocardiographic markers of diastolic dysfunction. *Circ Arrhythmia Electrophysiol*. 2012;5:537–543. doi: 10.1161/CIRCEP.111.969717
12. Lumens J, Arts T, Tim Marcus J, Vonk-Noordegraaf A, Delhaas T. Early-diastolic left ventricular lengthening implies pulmonary hypertension-induced right ventricular decompensation. *Cardiovasc Res*. 2012;96:286–295. doi: 10.1093/cvr/cvs251
13. Hardziyenka M, Campian ME, Bouma BJ, Linnenbank AC, de Bruin-Bon HACMR, Kloek JJ, van der Wal AC, Baan J, de Beaumont EM, Reesink HJ, et al. Right-to-left ventricular diastolic delay in chronic thromboembolic pulmonary hypertension is associated with activation delay and action potential prolongation in right ventricle. *Circ Arrhythmia Electrophysiol*. 2009;2:555–561. doi: 10.1161/CIRCEP.109.856021
14. Andersen S, Nielsen-Kudsk JE, Noordegraaf AV, de Man FS. Right ventricular fibrosis. *Circulation*. 2019;139:269–285. doi: 10.1161/CIRCULATIONAHA.118.035326
15. Tanaka Y, Takase B, Yao T, Ishihara M. Right ventricular electrical remodeling and arrhythmogenic substrate in rat pulmonary hypertension. *Am J Respir Cell Mol Biol*. 2013;49:426–436. doi: 10.1165/rcmb.2012-0089OC
16. Swift AJ, Capener D, Johns C, Hamilton N, Rothman A, Elliot C, Condliffe R, Charalampopoulos A, Rajaram S, Lawrie A, et al. Magnetic resonance imaging in the prognostic evaluation of patients with pulmonary arterial hypertension. *Am J Respir Crit Care Med*. 2017;196:228–239. doi: 10.1164/rccm.201611-2365OC
17. Lewis RA, Johns CS, Cogliano M, Capener D, Tubman E, Elliot CA, Charalampopoulos A, Sabroe I, Thompson AAR, Billings CG, et al. Identification of cardiac magnetic resonance imaging thresholds for risk stratification in pulmonary arterial hypertension. *Am J Respir Crit Care Med*. 2020;201:458–466. doi: 10.1164/rccm.201909-1771OC
18. Abman SH, Hansmann G, Archer SL, Ivy DD, Adatia I, Chung WK, Hanna BD, Rosenzweig EB, Raj JU, Cornfield D, et al. Pediatric pulmonary hypertension. *Circulation*. 2015;132:2037–2099. doi: 10.1161/CIR.0000000000000329
19. Ivy DD, Abman SH, Barst RJ, Berger RMF, Bonnet D, Fleming TR, Haworth SG, Raj JU, Rosenzweig EB, Schulze Neick I, et al. Pediatric pulmonary hypertension. *J Am Coll Cardiol*. 2013;62. doi: 10.1016/j.jacc.2013.10.028
20. Rijnbeek PR, Witsenburg M, Schrama E, Hess J, Kors JA. New normal limits for the paediatric electrocardiogram. *Eur Heart J*. 2001;22:702–711. doi: 10.1053/euhj.2000.2399
21. Prenner SB, Shah SJ, Goldberger JJ, Sauer AJ. Repolarization heterogeneity: beyond the QT interval. *J Am Heart Assoc*. 2016;5:e003607. doi: 10.1161/JAHA.116.003607
22. Meijborg VMF, Conrath CE, Opthof T, Belterman CNW, De Bakker JMT, Coronel R. Electrocardiographic T wave and its relation with ventricular repolarization along major anatomical axes. *Circ Arrhythmia Electrophysiol*. 2014;7:524–531. doi: 10.1161/CIRCEP.113.001622
23. Nagueh SF, Smiseth OA, Appleton CP, Byrd MF III, Dokainish H, Edvardsen T, Flachskampf FA, Gillebert TC. Recommendations for the evaluation of left ventricular diastolic function by echocardiography: an update from the American Society of Echocardiography and the European Association of Cardiovascular Imaging. *J Am Soc Echocardiogr*. 2016;2016:277–314. doi: 10.1016/j.echo.2016.01.011
24. Flachskampf FA, Biering-Sorensen T, Solomon SD, Duvernoy O, Bjerner T, Smiseth OA. Cardiac imaging to evaluate left ventricular diastolic function. *JACC Cardiovasc Imaging*. 2015;8:1071–1093. doi: 10.1016/j.jcmg.2015.07.004
25. Jone P-N, Schäfer M, Pan Z, Bremen C, Ivy DD. 3D echocardiographic evaluation of right ventricular function and strain: a prognostic study in paediatric pulmonary hypertension. *Eur Hear J–Cardiovasc Imaging*. 2017;19:1–8. doi: 10.1093/ehjci/jex205
26. Janoušek J, Kovanda J, Ložek M, Tomek V, Vojtovič P, Gebauer R, Kubuš P, Krejčíř M, Lumens J, Delhaas T, et al. Pulmonary right ventricular resynchronization in congenital heart disease: acute improvement in right ventricular mechanics and contraction efficiency. *Circ Cardiovasc Imaging*. 2017;10:1–9. doi: 10.1161/CIRCIMAGING.117.006424
27. Burkett DA, Slorach C, Patel SS, Redington AN, Ivy DD, Mertens L, Younoszai AK, Friedberg MK. Impact of pulmonary hemodynamics and ventricular interdependence on left ventricular diastolic function in children with pulmonary hypertension. *Circ Cardiovasc Imaging*. 2016;9:1–12. doi: 10.1161/CIRCIMAGING.116.004612
28. Burkett DA, Slorach C, Patel SS, Redington AN, Ivy DD, Mertens L, Younoszai AK, Friedberg MK. Left ventricular myocardial function in children with pulmonary hypertension: relation to right ventricular performance and hemodynamics. *Circ Cardiovasc Imaging*. 2015;8. doi: 10.1161/CIRCIMAGING.115.003260
29. Knight DS, Steeden JA, Moledina S, Jones A, Coghlan JG, Muthurangu V. Left ventricular diastolic dysfunction in pulmonary hypertension predicts functional capacity and clinical worsening: a tissue phase mapping study. *J Cardiovasc Magn Reson*. 2015;17:116. doi: 10.1186/s12968-015-0220-3
30. Liles JT, Hoyer K, Oliver J, Chi L, Dhalla AK, Belardinelli L. Ranolazine reduces remodeling of the right ventricle and provoked arrhythmias in rats

with pulmonary hypertension. *J Pharmacol Exp Ther*. 2015;353:480–489. doi: 10.1124/jpet.114.221861
31. Tanaka Y, Takase B, Yao T, Ishihara M. Right ventricular electrical remodeling and arrhythmogenic substrate in rat pulmonary hypertension. *Am J Respir Cell Mol Biol*. 2013;49:426–436. doi: 10.1165/rcmb.2012-0089OC
32. Spragg DD, Akar FG, Helm RH, Tunin RS, Tomaselli GF, Kass DA. Abnormal conduction and repolarization in late-activated myocardium of dyssynchronously contracting hearts. *Cardiovasc Res*. 2005;67:77–86. doi: 10.1016/j.cardiores.2005.03.008
33. Schäfer M, Bjornstad P, Frank BS, Baumgartner A, Truong U, Enge D, von Alvensleben JC, Mitchell MB, Ivy DD, Barker AJ, et al. Frequency of reduced left ventricular contractile efficiency and discoordinated myocardial relaxation in patients aged 16 to 21 years with type 1 diabetes mellitus (from the Emerald Study). *Am J Cardiol*. 2020;128:45–53. doi: 10.1016/j.amjcard.2020.04.041
34. Zhu TG, Patel C, Martin S, Quan X, Wu Y, Burke JF, Chernick M, Kowey PR, Yan G-X. Ventricular transmural repolarization sequence: its relationship with ventricular relaxation and role in ventricular diastolic function. *Eur Heart J*. 2008;30:372–380. doi: 10.1093/eurheartj/ehn585
35. Dragulescu A, Mertens L, Friedberg MK. Interpretation of left ventricular diastolic dysfunction in children with cardiomyopathy by echocardiography: problems and limitations. *Circ Cardiovasc Imaging*. 2013;6:254–261. doi: 10.1161/CIRCIMAGING.112.000175